# A Novel, More Efficient Approach to Generate Bioactive Inhibins

Kelly L. Walton, Emily K. Kelly, Katharine E. Johnson, David M. Robertson, Peter G. Stanton, and Craig A. Harrison

Hudson Institute of Medical Research, Clayton, Victoria 3168, Australia

Gonadal-derived inhibins are essential factors in mammalian reproduction, negatively regulating pituitary production of FSH. Interestingly, declines in inhibin levels across the menopause transition correlate with not only an increase in FSH but also a rapid decrease in bone mass. Therefore, inhibins have been touted as potential therapeutics for osteoporosis in postmenopausal women. However, as heterodimeric proteins of $\alpha$- and $\beta$- ($\beta_A$ or $\beta_B$)-subunits, inhibins are difficult to produce recombinantly, are poorly processed to their mature bioactive forms, and their expression is always accompanied by production of activins ($\beta$-subunit homodimers), the proteins they antagonize. In this study, we developed the methodology to circumvent most of these issues. Initially, the cleavage sites between the pro- and mature domains of the $\alpha$- and $\beta_A$-subunits were modified to ensure complete processing. These modifications led to a marked increase (9-fold) in the levels of bioactive inhibin A and a striking decrease (12.5-fold) in mature activin A production. Next, a single point mutation (M418A) was incorporated into the $\beta_A$-subunit, which reduced residual activin activity approximately 100-fold and, in so doing, increased inhibin bioactivity 8-fold. Finally, we showed that inhibin A noncovalently associated with its prodomain was more potent (~20-fold) than mature inhibin A in specific in vitro bioassays, indicating an important role of the prodomain in inhibin bioactivity. In conclusion, the production of potent inhibin analogs in the virtual absence of activin activity will greatly facilitate the investigation of the therapeutic potential of these gonadal hormones on bone and other tissues. **(*Endocrinology* 157: 2799–2809, 2016)**

FSH regulates spermatogenesis in males and folliculogenesis in females. In response to FSH, testicular Sertoli cells and ovarian granulosa cells produce inhibin A and/or inhibin B, which target the gonadotrope cells of the pituitary to down-regulate the production and secretion of FSH in a cycle-dependent manner in females and in a tonic pattern in males (1). Circulating inhibin levels decrease dramatically across the menopause transition and inversely correlate with increased serum FSH (2).

Inhibins A and B are unique members of the TGF-$\beta$ superfamily as 1) they are heterodimers composed of $\alpha$- and $\beta$ ($\beta_A$ or $\beta_B$)-subunits, whereas most other family members are homodimers; 2) they act as antagonists, rather than agonists, inhibiting signaling of activin-related proteins; and 3) they function in an endocrine rather than autocrine/paracrine manner. These aspects of inhibin biology are crucial for their roles in reproduction, but they also endow these hormones with the potential to regulate additional physiological processes, including bone and muscle growth.

Analogous to other members of the TGF-$\beta$ superfamily, inhibin $\alpha$- and $\beta$-subunits are synthesized as large precursor molecules with the N-terminal prodomains mediating the folding and dimerization of the C-terminal mature domains (3). Dimeric precursors are cleaved by proprotein convertases and inhibins are secreted from Sertoli and granulosa cells noncovalently associated with their prodomains (pro-mature complexes). Once localized to target tissues, the prodomains are likely to be displaced, enabling mature 31-kDa inhibins to associate with their cognate receptors.

ISSN Print 0013-7227 ISSN Online 1945-7170
Printed in USA

Received November 16, 2015. Accepted April 4, 2016.
First Published Online April 7, 2016

**For News & Views see page 2583**

Abbreviations: ActRII, activin type II receptor; ALK, activin receptor-like kinase; FCS, fetal calf serum; HEK, human embryonic kidney; HRP, horseradish peroxidise; IMAC, immobilized metal ion affinity chromatography; mAb, monoclonal antibody; SCUT, supercut; Smad, phosphorylated mothers against decapentaplegic; TBS-T, Tris-buffered saline with Tween-20.

It is recognized that inhibins A and B regulate FSH secretion from the anterior pituitary by blocking the stimulatory actions of activins (4). Activins are dimers of inhibin β-subunits: $\beta_A$-$\beta_A$ (activin A), $\beta_B$-$\beta_B$ (activin B,) and $\beta_A$-$\beta_B$ (activin A/B). Activins initially bind to type II receptors, ActRIIA or ActRIIB, leading to recruitment, phosphorylation, and activation of the type I receptor, (activin receptor-like kinase [ALK]-4). Activated ALK4 phosphorylates intracellular signaling molecules, phosphorylated mothers against decapentaplegic (Smad)-2/3, which in turn form a complex with the coactivator, Smad4. The resulting Smad oligomer localizes within the nucleus to regulate target genes (eg, *Fshb*) in a cell- and context-dependent manner (5). Inhibin antagonism of activin-related ligands is dependent on interactions with betaglycan, a cell-surface proteoglycan that also acts as a TGF-β coreceptor (6). Betaglycan binds inhibins A and B directly and promotes the formation of a stable high-affinity complex involving activin type II receptors (6). Sequestration of type II receptors in this way prevents their interactions with signaling ligands such as activins. In the absence of betaglycan, inhibin cannot effectively block activin-mediated FSH secretion by pituitary gonadotrope cells (7).

The widespread expression of betaglycan and ActRIIA/B together with the fact that activins target multiple tissues suggest that inhibin's actions extend beyond the negative regulation of FSH. Indeed, serum inhibins A and B levels correlate inversely with markers of bone formation and bone resorption in women across the menopause transition, and it has been proposed that these decreases in inhibin contribute to the initial bone loss during this period (8). Significantly, when applied to in vivo models of bone degeneration, inhibin A has been shown to rescue bone growth (9, 10). Thus, gonadal inhibins are likely components of the normal endocrine repertoire that regulate not only reproductive function but also bone health.

Definitively characterizing the physiological roles of inhibin A and B, however, has proven difficult for several reasons. First, targeted deletion of the inhibin α-subunit in mice leads to unopposed gonadal expression of activins A and B. Because activins, in combination with gonadotropins, stimulate granulosa and Sertoli cell proliferation, inhibin-deficient mice develop sex-cord stromal tumors with 100% penetrance, as early as 4 weeks of age (11). As tumors progress, serum levels of activins A and B increase up to 500-fold (12), and mice die from a cachexia-like wasting syndrome between 12 and 17 weeks (13). Thus, the phenotype of the inhibin α-subunit knockout mouse does not really reflect the loss of inhibin but rather the devastating systemic effects of elevated circulating activins. Second, in vivo overexpression of inhibins (α/β-subunit heterodimers) is always accompanied by the production of activins (β-subunit homodimers), which have pleiotropic effects in multiple organs (14). Finally, recombinant production of inhibins and their separation from contaminating activins is difficult, and the resultant 31-kDa mature inhibin forms have short in vivo half-lives (15).

Here we describe a new expression system for the production of bioactive inhibin A, in the virtual absence of contaminating activins. Moreover, we show that inhibin A noncovalently associated with its prodomain (proinhibin A) has enhanced activity and that this complex can be readily purified. Our new production and streamlined purification system makes it feasible to finally explore the therapeutic potential of inhibins A and B on bone and other tissues.

## Materials and Methods

### Generation of mutant inhibins

The cleavage sites intervening the pro- and mature domains in the inhibin α- and $\beta_A$-subunits were modified using site-directed mutagenesis. A pCDNA3.1 vector (Life Technologies) containing either the full-length wild type human inhibin α-subunit (sequence reference NM_002191.3) or the $\beta_A$-subunit (sequence reference NM_002192.2) served as the templates in these reactions. The native furin cleavage sites (RXXR) were replaced with an ideal theoretical site (ISSRKKRSVSS) (16) to enhance the processing of proinhibin forms. This was achieved by overlap extension PCR, using designed supercut (SCUT) primers in combination with primers flanking the ORFs (primer details provided in Supplemental Table 1) to enable cloning into compatible sites of pCDNA3.1. To aid purification, a polyhistidine tag was inserted at a previously determined permissive site (17), immediately prior to the pro- and mature domain cleavage site. This was achieved using poly-HIS-tag primers in combination with flanking primers as outlined in Supplemental Table 1, to enable cloning into pCDNA3.1. Finally, the M418A (M108A in mature region) mutation in the inhibin $\beta_A$-subunit was generated using M418A primers (Supplemental Table 1) with the Quik Change Lightning site-directed mutagenesis kit (Agilent Technologies). All constructs were verified by DNA sequencing.

Inhibin variants were produced by transient transfection in human embryonic kidney (HEK293T) cells using Lipofectamine 2000 (Life Technologies). In brief, cells were plated at $8 \times 10^5$ cells/well in six-well plates. Wild-type or mutant α-subunit constructs were combined with $\beta_A$-subunit variants, and Lipofectamine 2000 was added according to the manufacturer's instructions. After a 20-minute incubation, DNA/Lipofectamine complexes were added directly to the plated cells and incubated in serum-free Opti-MEM medium (Life Technologies) for a further 48 hours at 37°C in 5% $CO_2$.

Western blotting was used to assess inhibin and activin forms in the conditioned medium from transfected HEK293T cells. At 48 hours after transfection, conditioned medium was

combined with 4× LDS loading dye (Life Technologies), and nonreduced samples were separated by 10% SDS-PAGE. After electrophoresis, samples were transferred onto ECL Hybond membranes (GE Healthcare). Membranes were blocked for a minimum of 1 hour in 1% BSA in Tris-buffered saline with 0.05% Tween-20 (TBS-T). Inhibin forms were detected using monoclonal antibodies (mAbs) to the inhibin $\beta_A$- (E4, binds residues 401–413 [18]), or $\alpha$-subunit (R1, binds residues 233–264 [18]). The E4 antibody was obtained from Beckman Coulter or Oxford Brookes University and requires an antigen retrieval step during incubation (6% $H_2O_2$). Antibodies were incubated in 1% BSA/TBS-T for 2 hours and excess antibody removed by multiple washes with TBS-T. Bound R1 and E4 antibodies were then detected by incubation with a mouse secondary antibody conjugated to horseradish peroxidase (mouse IgG-horseradish peroxidase [HRP]; GE Lifesciences). After multiple washes, chemiluminescence was measured using Lumilight substrates (Roche Applied Sciences) and a Bio-Rad Chemidoc XRS system (Bio-Rad Laboratories) (Table 2).

## Quantification of inhibin

Inhibin A levels were determined based on the method of Groome et al (18) with modification (17). This ELISA uses the $\beta_A$-subunit mAb (E4) as a capture antibody and $\alpha$-subunit mAb (R1) as the label. Samples and standards were first diluted in a low-Triton assay buffer (10 mM Tris-HCl, 154 mM NaCl, 0.1% Triton X-100, 1% BSA) and then oxidized using 1% $H_2O_2$ (final concentration). The samples were loaded into E4 coated 96-well plates and incubated overnight at room temperature. Bound inhibin was labeled using biotinylated-R1 antibody diluted in the low-Triton assay buffer. After R1 labeling, plates were treated with streptavidin-HRP and then washed and developed with 3,3′,5,5′-tetramethylbenzidine substrate (Life Technologies). The ELISA was stopped using 0.1 M $H_2SO_4$, and absorbance determined at 450 nM on a SpectraMax plate reader (Molecular Devices). Assay sensitivity was 6 pg/mL. Purified 34-kDa inhibin A generated by our laboratory was used as a reference standard (19).

## Quantification of activin

Activin A standard and samples (diluted in 5% BSA in PBS, pH 7.4) were treated with sodium dodecyl sulfate (final concentration 3%) and boiled for 3 minutes. Once cooled, samples were treated with $H_2O_2$ (final concentration 2%) and incubated for 30 minutes at room temperature. Samples were added to E4 antibody-coated plates and incubated for 1 hour at room temperature. Bound activins were detected by probing with biotinylated-E4 antibody and incubated overnight at room temperature. After washing, a streptavidin-HRP conjugate was added to the wells and incubated at room temperature for 1 hour. After further washes, HRP activity was detected as described above.

## Production and purification of inhibins by immobilized metal ion affinity chromatography (IMAC)

Proinhibin forms were produced by transient transfection in HEK293T cells using Lipofectamine 2000 (Life Technologies). In brief, cells were plated at $11 \times 10^6$ cells/plate on 15-cm plates and then transfected with 3:2 ratio of inhibin $\alpha$- and $\beta$-subunit DNA constructs using Lipofectamine 2000 and Opti-MEM media (according to the manufacturer's protocol; Life Technologies). Proinhibin was then isolated from conditioned media by IMAC immunoaffinity. Conditioned media (100 mL) was first concentrated (twice) using centricon devices with a 5-kDa molecular mass cutoff (EMD Millipore) and resuspended in phosphate buffer (10 mM $PO_4$; 0.5 M NaCl, pH 8.0). Concentrated media were applied to a HisPur cobalt-resin (Thermo Fisher Scientific) and incubated overnight at 4°C. Unbound protein was collected, and the resin washed four times with phosphate buffer. Bound inhibins were eluted with 150 mM imidazole in phosphate buffer. Imidazole was removed by buffer exchange on a PD-10 column (GE Healthcare), and PBS (pH 7.4) with 0.1% BSA was applied to the preparations. IMAC purification was performed twice to enrich inhibins and deplete contaminating activin forms. The recovery and yield of proinhibin preparations were determined by Western blot analysis (using R1 MAb) and an inhibin A ELISA, as described above.

## Separation of inhibin and activin forms by gel filtration

The final inhibin preparations were found to contain low levels of activin. To establish the contribution of activin toward inhibin bioactivity, the activins were first removed using gel filtration. In brief, 1–2 $\mu$g of IMAC purified protein was applied to a HiLoad 16/60 Superdex 200 size exclusion column (GE Healthcare), and the proteins were eluted in 0.1 M phosphate (pH 7.4). Inhibin A and activin A ELISAs (described above) were used to identify the fractions containing predominantly inhibins along with Western blots using antibodies directed toward the inhibin $\alpha$-subunit (R1) and $\beta$A-subunits (E4). These fractions were pooled and concentrated using Centricon devices prior to bioactivity assessment in the L$\beta$T2 bioassay.

## Determination of inhibin bioactivity using FSH in vitro bioassays

Animal experiments were conducted under the Monash Medical Centre Animal Ethics Code (MMCB 2012/37). The ability of the inhibin preparations to suppress activin-induced FSH release was examined in cultured rat pituitary cells (20) and in a mouse pituitary gonadotrope cell line (L$\beta$T2). For the rat pituitary culture bioassay, the anterior pituitary glands of adult male Sprague Dawley rats (12 wk) were enzymatically dispersed with trypsin and plated at 50 000 cells/well in 48-well plates in DMEM-Fl2 (Life Technologies) containing 10% fetal calf serum (FCS). After incubation at 37°C in 5% $CO_2$ for 48 hours, cells were washed with DMEM-F12 containing 0.1% BSA and incubated for a further 4 hours. Cells were then treated with increasing doses of inhibin A (5–800 pM) diluted in DMEM-F12 media with 0.1% BSA. After 48 hours, the cell media were assayed for rat FSH by a specific rat FSH immunofluorometric assay (21) using reagents kindly provided by A. Grootenhuis and J. Verhagen (N.V. Organon). The sensitivity of the in vitro bioassay was 75 pg/well using the highly purified 31-kDa inhibin A preparation (19).

For the L$\beta$T2 cell in vitro bioassay, cells were plated in 48-well plates at a density of $2.5 \times 10^5$ cells/well. The cells were allowed to recover for 24 hours in DMEM supplemented with 10% FCS and then treated with 150 pM activin A in the presence of increasing concentrations of inhibin (0.1–90 nM). After 24

hours of incubation, the media were collected for the FSH assay, as described above.

### Smad phosphorylation

The ability of proinhibin A to suppress activin-induced Smad2 phosphorylation, relative to mature inhibin A, was determined in LβT2 cells. Cells were seeded at $2 \times 10^6$ cells/well in polylysine coated six-well plates. The following day, the media were changed to DMEM, 0.2% FCS, and 50 mM HEPES, containing 150 pM activin A with increasing concentrations of inhibin (0.3–3 nM). After 30 minutes of treatment, cells were washed with PBS and lysed in 100 μl radioimmunoprecipitation assay buffer (50 mM Tris; 0.9% NaCl, pH 8.0; 1% Nonidet P-40; 0.5% deoxycholic acid; 0.1% sodium dodecyl sulfate), containing protease inhibitor cocktail tablets (Roche Applied Sciences) and phosphatase inhibitors. Lysates were collected, clarified by centrifugation, and combined with reducing sample buffer (Life Technologies) and analyzed by Western blot. Phospho-Smad2 and Smad2 (Cell Signaling Technologies) antibodies were used at 1:2000 dilutions. Bound primary antibodies were detected using goat antirabbit or sheep antimouse horseradish peroxidise conjugates (GE Healthcare Life Sciences). These studies were undertaken on duplicate cultures.

### Assessment of inhibin binding to betaglycan

The ability of proinhibin A to displace inhibin binding to betaglycan was determined by a binding assay in HEK293T cells. In brief, HEK293T cells were plated at $10^5$ cells/well in DMEM and 10% FCS in 24-well plates coated with poly-D-lysine and incubated for 48 hours at 37°C. The following day, cells were transfected with 10 ng/well of a truncated form of betaglycan (BG 576-853 [22]) using Lipofectamine 2000 (Life Technologies) and incubated overnight. Cells were then washed in binding buffer (DMEM and 0.1% BSA) and incubated for 4 hours at room temperature with $^{125}$I-inhibin A (40 000 cpm/well) (23) together with increasing concentrations of inhibin forms (1–40 nM). The cells were washed in 10 mM PBS (pH 7.4) and solubilized in 1% Triton X-100. Radioactivity was measured using a γ counter (Laboratory Technologies, Inc). The binding data were analyzed using the Prism program (version 6.0; GraphPad Software).

### Data analysis

One-way ANOVAs were used to assess statistical differences relative to wild-type inhibins/activins, with the Dunnett test used for comparisons between the specific group means, using GraphPad Prism version 6 (GraphPad Software). Significance is represented as follows: *, $P < .05$ and **, $P < .01$. Data are presented as the means ± SD.

## Results

### Enhanced processing of the α-subunit favors inhibin production over activin

The inhibin α- and β-subunits comprise an N-terminal prodomain and a C-terminal mature domain, separated by a proprotein convertase cleavage site (Figure 1A). After dimerization, the mature inhibin ligand is enzymatically released from its prodomains, enabling bioactivity. However, recombinant production of inhibin A indicates that processing by members of the proprotein convertase family is inefficient because significant amounts of unprocessed inhibin A and full-length, 50-kDa α-subunit are present in conditioned media, with relatively little mature 31- to 34-kDa inhibin A (Figure 1B, lane 1). Further confounding inhibin production/purification are the high levels of mature activin A that are coproduced when HEK293T cells are transfected with wild-type α- and $\beta_A$-subunits (Figure 1C, lane 1). To improve enzymatic processing of the α-subunit, we replaced the endogenous cleavage site ($^{229}$RARR$^{232}$) with an ideal proprotein convertase cleavage site ($^{229}$ISSRKKRSVS$^{238}$) (Figure 1A) and expressed this supercut variant ($SCUT_{S1}$) in HEK293F cells. The SCUT form of the inhibin α-subunit resulted in a marked increase in the levels of inhibin A (Figure 1B, lane 2) and a surprising decrease in mature activin A production (Figure 1C, lane 2). Specific ELISAs identified similar changes in total inhibin and activin levels (Figure 1, D and E).

Subsequently, we introduced the same enhanced cleavage site into the $\beta_A$-subunit and showed that in combination with the wild-type α-subunit, this modification also increased mature inhibin A production (Figure 1B, lane 3), although mature activin A levels were not altered (Figure 1C, lane 3). The apparent increase in mature inhibin A production was not accurately represented in the inhibin ELISA (Figure 1D), as a result of this assay capturing both mature and precursor inhibin A forms. Combining SCUT versions of both the α- and $\beta_A$-subunits led to nearly complete processing of precursor proteins and the greatest proportional ratio of inhibin to activin production (69:1) (Table 1). These results support the concept that processing of the α-subunit is the limiting step in inhibin production, relative to activin.

### Overexpressing the α-subunit greatly increases inhibin production

In our initial experiments, HEK293T cells were transfected with an equal ratio of SCUT α- and $\beta_A$-subunit DNA. Varying this ratio (from 4:1 to 1:4) had interesting effects on inhibin and activin production (Supplemental Figure 1). At a 4:1 or 3:2 ratio of α:$\beta_A$-subunit, mature inhibin A levels were relatively high (Supplemental Figure 1, A and C), whereas mature activin A levels were negligible (Supplemental Figure 1, B and D). Interestingly, when the transfection ratio favored $\beta_A$-subunit expression (2:3 or 1:4 ratio of α:$\beta_A$-subunit) 3- to 4-fold higher levels of mature inhibin A were actually produced (Supplemental Figure 1, A and C). However, increased $\beta_A$-subunit expression was also accompanied by significant activin

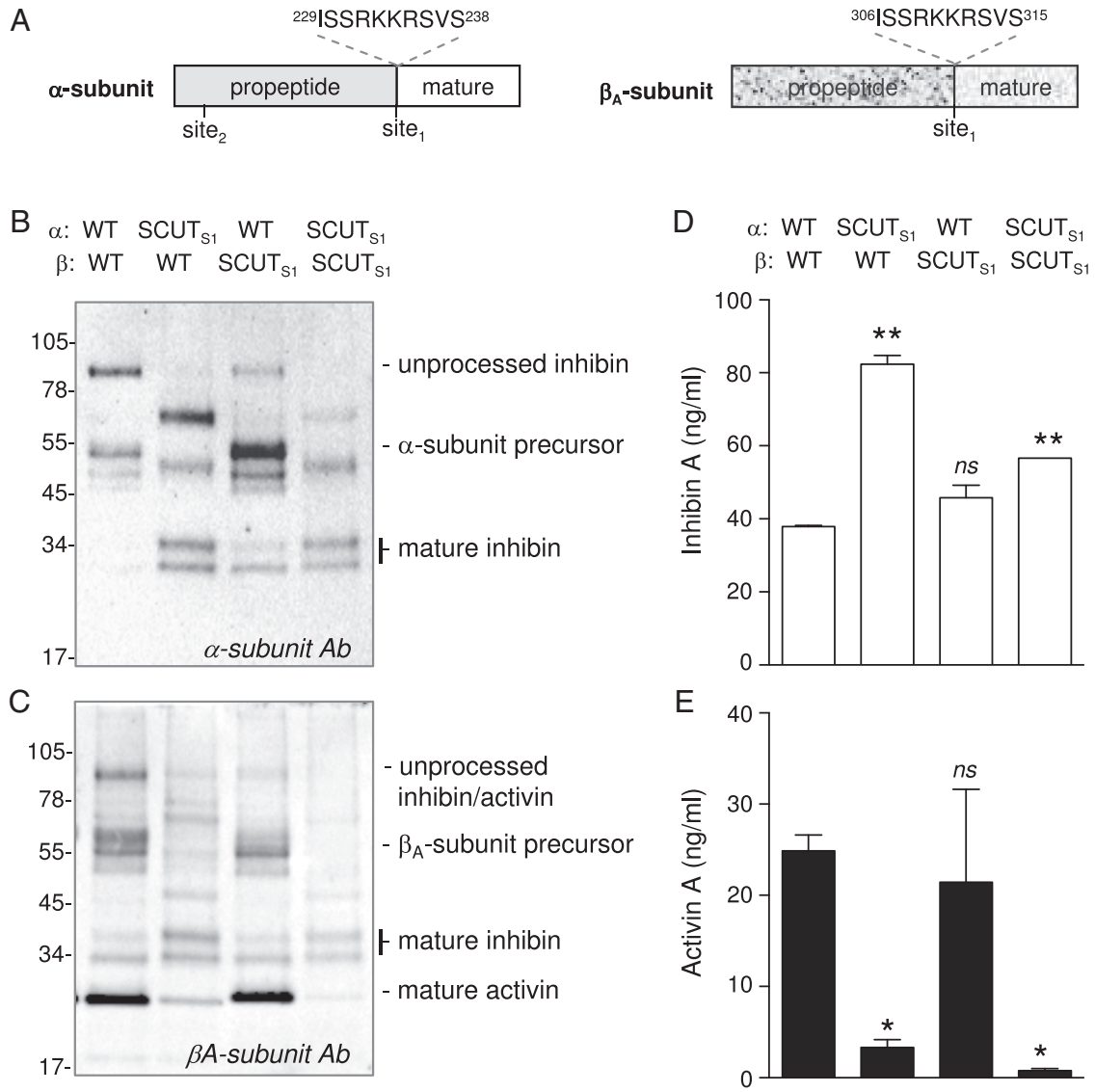


**Figure 1.** Effect of enhanced subunit processing on inhibin/activin production in mammalian cells. A, The native cleavage sites (RXXR) in the inhibin $\alpha$- and $\beta$-subunits were enhanced by site-directed mutagenesis. B and C, Wild-type (WT) or supercut (*SCUT*$_{S1}$, where *S1* refers to cleavage site$_1$ intervening the promature domains) inhibin $\alpha$- and $\beta_A$-subunits were cotransfected into HEK293F cells, and the resultant inhibin and activin forms produced were assessed by Western blot, using antibodies to the $\alpha$- and $\beta_A$-subunits (R1 and E4, respectively). D and E, Specific ELISAs were used to quantitate inhibin and activin produced by HEK293F cells. Results are representative of three experiments. *, $P < .05$; **, $P < .01$, ns, not significant.

production (Supplemental Figure 1, B and D). Therefore, we chose a 3:2 ratio of $\alpha$:$\beta_A$-subunit for all subsequent experiments.

**Table 1.** Ratio of Inhibin to Activin Produced After Transient Transfection of HEK293F Cells With Wild-Type and SCUT Constructs

| $\alpha$-Subunit | $\beta$A-Subunit | Ratio Inhibin to Activin (Mean ± SD) |
|---|---|---|
| WT | WT | 1.5 ± 0.7 |
| SCUT | WT | 24.8 ± 0.3 |
| WT | SCUT | 2.2 ± 0.3 |
| SCUT | SCUT | 68.7 ± 7.3 |

Abbreviation: WT, wild type.

## Modifying the secondary cleavage site in the $\alpha$-subunit further enhances inhibin A production

When we commenced large-scale production of inhibin A using the modified $\alpha$- and $\beta_A$-subunit constructs, we noted an increase in the free 50-kDa $\alpha$-subunit (Figure 2B) relative to the earlier small-scale transfections (Figure 1B). The $\alpha$-subunit prodomain has a second cleavage site at the N terminus (Figure 2A), which we have previously shown is critical for inhibin production (24). Here we replaced this secondary cleavage site ($^{56}$RRLPRR$^{61}$) with an improved proprotein convertase cleavage site ($^{56}$RRRRRR$^{61}$) (Figure 2A) and expressed this supercut-2 (SCUT$_{S2}$) variant together with the modified $\beta_A$-subunit in HEK293T cells. Western analysis showed that these modifications abrogated expression of the

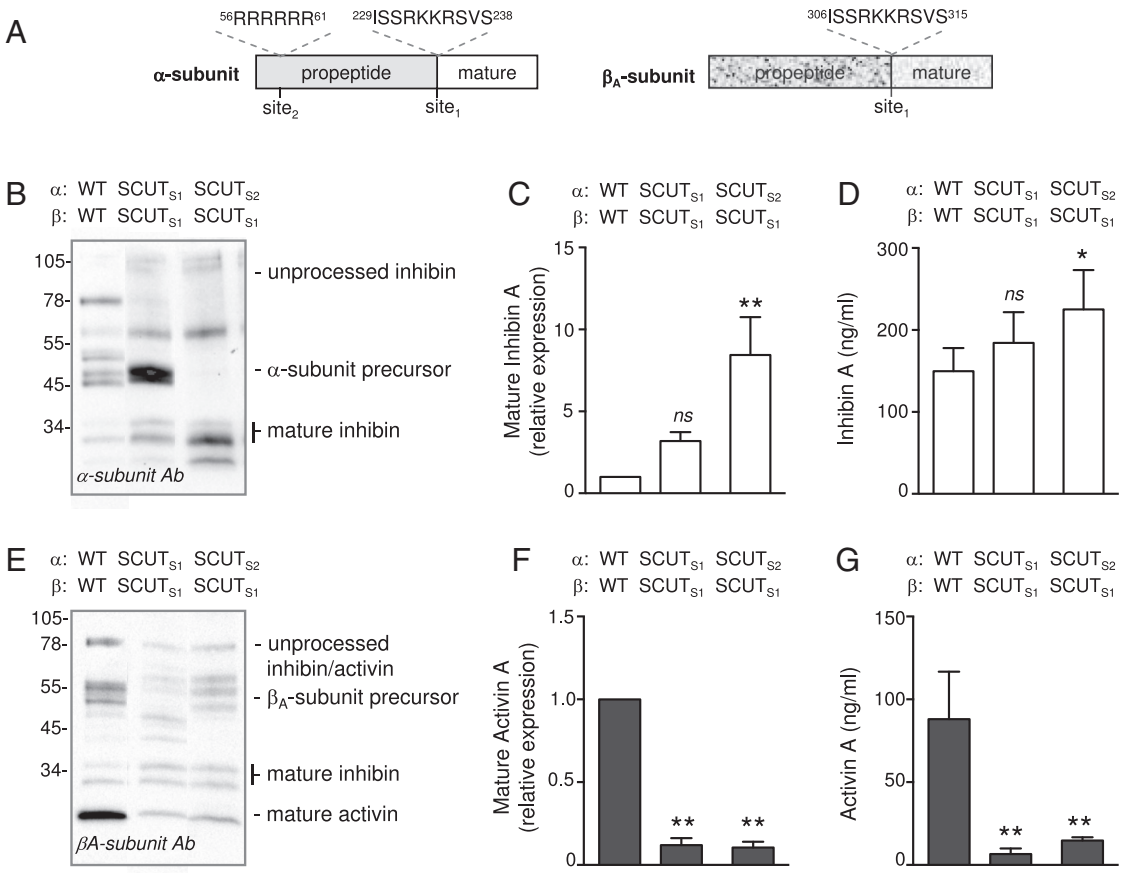


**Figure 2.** Enhanced processing within the inhibin α-subunit prodomain favors the production of mature inhibins. A, The inhibin α-subunit uniquely contains a second processing site ($site_2$) within its prodomain. This cleavage site was enhanced by targeted mutagenesis alongside $site_1$, which intervenes the pro- and mature domains. B and E, Wild-type (WT) or SCUT inhibin α- and $\beta_A$-subunits were cotransfected into HEK293T cells, and the resultant inhibin and activin forms produced were assessed by Western blot ($SCUT_{S2}$ refers to α-subunit with both processing sites enhanced). C and F, Densitometry was used to determine the relative expression of mature (31 kDa) inhibin A and activin A, and total inhibin and activin forms were quantified by ELISAs (D and G). Results are average of three experiments. *, $P < .05$; **, $P < .01$.

free α-subunit and further increased mature inhibin A expression (Figure 2B, lane 3). Densitometry indicated that improving processing at both sites in the α-subunit increased mature inhibin production 9-fold relative to wild type and 2-fold relative to the initial SCUT variant (Figure 2C). Densitometric analysis proved to be a more accurate representation of mature inhibin levels in these samples because the ELISA failed to identify a clear significant trend (Figure 2D) (likely owing to the interference of multiple inhibin precursor forms in this assay). Mature activin A levels were 12.5-fold lower than wild type (Figure 2, E–G). Thus, improving both processing sites in the α-subunit results in a significant increase in mature inhibin A production and a corresponding decrease in activin A. The inhibin α-subunit $SCUT_{S2}$ and βA-subunit $SCUT_{S1}$ mutations were incorporated into all subsequent inhibin preparations in this study.

## Elimination of contaminating activin bioactivity by a single point mutation in the $\beta_A$-subunit

By improving the processing capacity of the inhibin α-subunit and optimizing the transfection ratio of α to $\beta_A$-subunit DNA, we greatly favored inhibin production over that of related activins. However, any residual activin A produced would retain bioactivity and therefore have the potential to counteract inhibins' effects. To eliminate contaminating activin bioactivity, a single-point mutation (M418A, or M108A in the mature region) was incorporated into the $\beta_A$-subunit at the type I receptor (ALK4) binding epitope (Figure 3A) (25). The M418A mutation did not affect the amounts of inhibin and activin produced by HEK293T cells (Figure 3, B and C); however, it resulted in an 8-fold increase in inhibin-like activity, as measured by the suppression of activin-induced FSH release by LβT2 mouse gonadotrope cells (Figure 3D). Two possibilities existed for the increased inhibin-like activity of the preparation: 1) loss of activin A activity after introduction of the M418A mutation or 2) gain of activin A (M418A) antagonistic activity, as previously described (25). To address the loss of activin activity, we transfected HEK293F cells with an activin-responsive luciferase reporter and treated cells with the inhibin A preparations. This assay

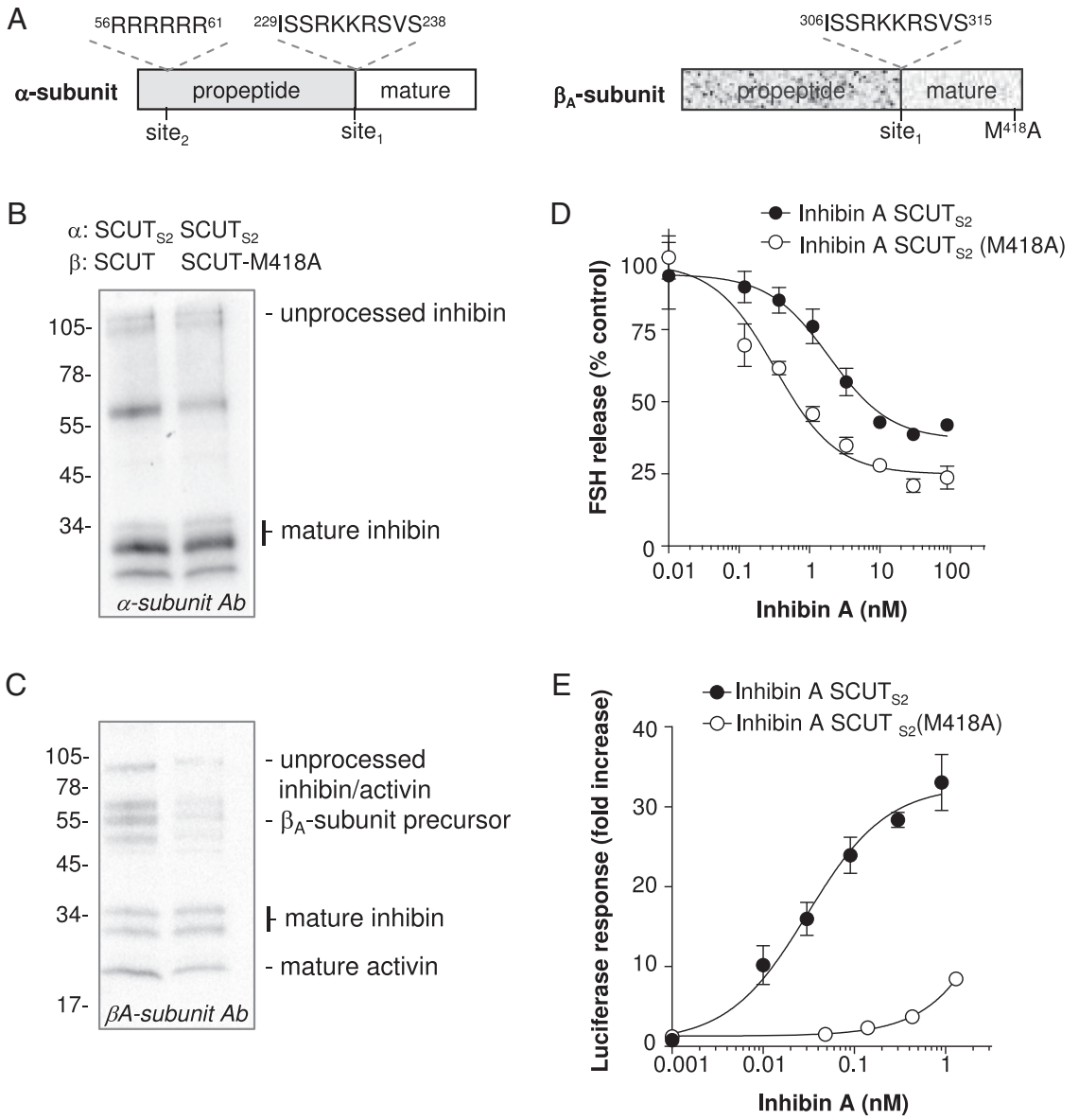


**Figure 3.** Inactivation of residual activin A improves inhibin bioactivity. A, An M418A mutation was incorporated into the $\beta_A$-subunit to inhibit activin binding to its type I receptor (ALK4). B and C, The effect of the M418A mutation on inhibin and activin biosynthesis was assessed by Western blot, using antibodies to the $\alpha$- and $\beta_A$-subunits (R1 and E4, respectively). D, The ability of inhibin M418A to suppress activin bioactivity was determined using an L$\beta$T2 gonadotrope FSH bioassay. The L$\beta$T2 cells were stimulated with 150 pM activin A and treated with increasing doses of either inhibin A-SCUT or inhibin A-SCUT (M418A). E, Activin bioactivity within the inhibin preparations was assessed using an activin-responsive luciferase reporter assay (A3-Luc). Transfected HEK293T cells were treated with increasing doses of inhibin preparations, and activity determined by measuring luciferase activity. Results are average of three experiments.

system is extremely sensitive to activin stimulation but does not respond to inhibin due to low betaglycan expression. Inhibin A-$SCUT_{S2}$ induced a dose-dependent increase in luciferase activity, confirming the presence of active activin A in this preparation, whereas inhibin A-$SCUT_{S2}$ (M418A) exhibited a 100-fold lower activin response (Figure 3E). Thus, a single-point mutation in the $\beta_A$-subunit further increases inhibin A-like activity by suppressing the ability of residual activin A to signal. We have previously shown, however, that activin (M418A) can act as an antagonist at high concentrations (25). Therefore, we used gel filtration chromatography to separate activin A (M418A) from inhibin A-$SCUT_{S2}$ (M418A) (Supplemental Figure 2). There was no change in inhibin-like activity following activin (M418A) removal (Supplemental Figure 2C), suggesting that the 8-fold increase in inhibitory activity of the preparation was primarily due to the loss of activin A activity.

## Purification of mature inhibin A

Recently numerous studies have shown that mature TGF-$\beta$ proteins are secreted from cells noncovalently as-

sociated with their prodomains (26–28). To determine whether proinhibin A was secreted as a noncovalent complex, a HIS tag was incorporated at the C terminus of the α-subunit prodomain immediately preceding the SCUT-processing site. Conditioned media from HEK293T cells transfected with HIS-tagged SCUT α-subunit ($SCUT_{S2}$) and SCUT $\beta_A$-subunit (M418A) was purified by IMAC affinity chromatography and analyzed by Western blot. More than 90% of mature inhibin A present in the starting material was copurified with the HIS-tagged prodomain (Figure 4, A and B), confirming that most inhibin A remains noncovalently associated with its prodomain upon secretion from the cell. Low levels of activin (M418A) were copurified with inhibin using this procedure (Figure 4, B and C), but this contaminating activin could be readily removed by gel filtration chromatography (Supplemental Figure 2). Interestingly, a silver-stained gel indicated that the eluate from the cobalt column was also very pure, containing almost entirely inhibin/activin precursor and mature forms (Supplemental Figure 3).

### Proinhibin A is a more potent activin antagonist than mature inhibin A in specific settings

Using FSH release assays in both primary rat pituitary cells and the LβT2 cell line, we compared the biological activity of IMAC-purified proinhibin A and HPLC-purified mature inhibin A (19). In primary pituitary cells, proinhibin A induced a dose-dependent decrease in FSH release ($IC_{50}$ 75 pM), which was similar to that observed with mature inhibin A ($IC_{50}$ 65 pM) (Figure 5A). Any possible influence of the prodomain in this assay system may have been masked by the very potent activity of inhibin A. Therefore, we repeated the comparison of the pro- and mature inhibin forms on activin-induced FSH release by LβT2 pituitary gonadotrope cells, which are less sensitive to inhibins, potentially as a result of lowered betaglycan expression (29). Remarkably, proinhibin A ($IC_{50}$ 45 pM) was 22-fold more potent than mature inhibin A ($IC_{50}$ 1 nM) in this assay system (Figure 5B). These differing activities were mirrored intracellularly in which mature inhibin A only partially blocked activin-induced Smad2 phosphorylation, whereas proinhibin A completely inhibited this response (Figure 5C). Mechanistically, it was found that proinhibin A ($IC_{50}$ 400 pM) was 5-fold more effective than mature inhibin ($IC_{50}$ 2 nM) at displacing $^{125}$I-inhibin A from cells transfected with betaglycan, suggesting that the prodomain increases inhibin's affinity for its coreceptor. Together these results indicate that in less responsive systems, inhibin A activity is significantly enhanced when noncovalently associated with its prodomain.

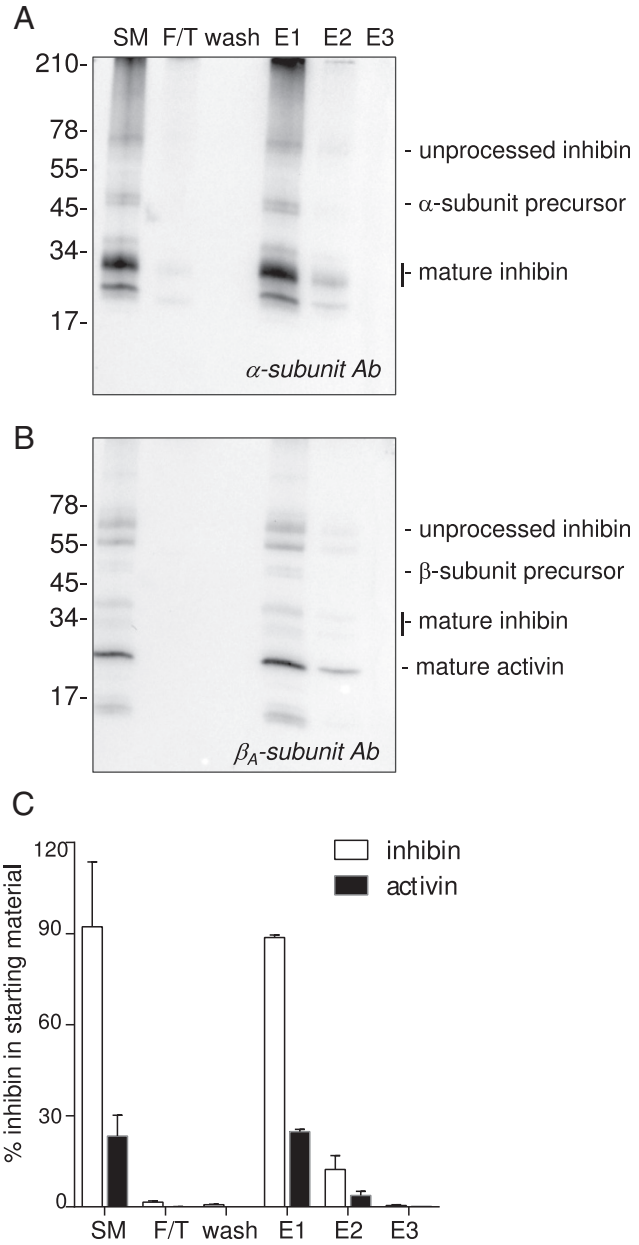


**Figure 4.** Purification of Inhibin A-SCUT (M418A) by affinity chromatography. Proinhibin A (comprising mutations α-$SCUT_{S2}$, βA-$SCUT_{S1}$/M418A) was purified using cobalt IMAC and recoveries assessed by Western blot using antibodies to the α- (A) and $\beta_A$-subunits (B). C, Inhibin A and activin A ELISAs were used to quantify the recoveries. Results are representative of three experiments; error is SD. SM, starting material; F/T, flow through; EL1–3, elutions 1–3.

## Discussion

The production and purification of inhibin in therapeutic amounts has proven difficult due to the inefficient processing of the heterodimeric precursor to the bioactive mature form and to the effort required to remove contaminating activins (19). To improve processing, we focused our attention on the inhibin α- and $\beta_A$-subunit prodomains. It is generally accepted within the TGF-β super-

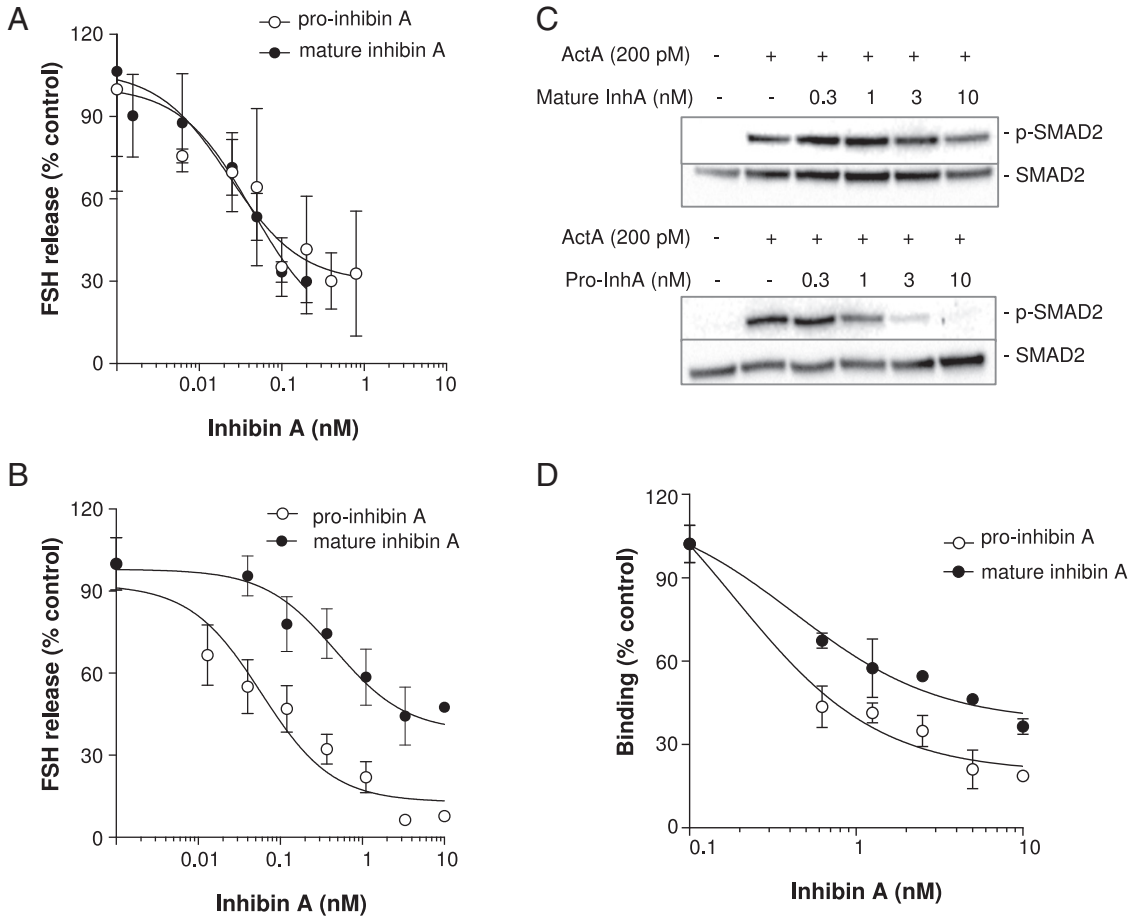


**Figure 5.** Analysis of proinhibin bioactivity. The ability of proinhibin A to suppress activin-induced FSH release was compared with mature inhibin A in both rat pituitary cell cultures (A) and mouse gonadotrope L$\beta$T2 cells (B). C, The ability of proinhibin A to suppress activin-induced SMAD2 phosphorylation was also assessed in L$\beta$T2 cells. Cells were treated with 150 pM activin A in the presence of increasing doses of proinhibin A or mature inhibin A. D, The ability of proinhibin and mature inhibin A to displace $^{125}$I-inhibin A binding to betaglycan was assessed in transfected HEK293T cells. Results are average of two to three experiments (Western blots are representative).

family that prodomains govern the correct folding of dimeric precursors within the endoplasmic reticulum (30). TGF-$\beta$ precursors then acquire complex carbohydrate modifications during exocytosis, indicating transit through the trans-Golgi network. Once the correct tertiary structure is achieved, TGF-$\beta$ precursors are proteolytically matured by proprotein convertases, either in a late Golgi compartment or extracellularly (30). For inhibin and activin, proprotein convertase-5/6 and furin have been identified as the processing enzymes (31, 32). However, the high levels of unprocessed inhibin and the low amounts of mature inhibin relative to activin, produced by HEK293T cells, suggested that $\alpha$-subunit processing is less efficient than that of the $\beta_A$-subunit. Therefore, we replaced the endogenous $\alpha$-subunit cleavage site ($^{229}$RARR$^{232}$) with an ideal proprotein convertase cleavage site ($^{229}$ISSRKKRSVS$^{238}$) (16). As anticipated, this modification significantly increased the amount of mature inhibin produced by HEK293T cells; however, it also resulted in a dramatic decrease in activin production. Because dimerization preceeds processing, this finding suggests that the SCUT site introduced into the $\alpha$-subunit induced a conformational change, which favored inhibin A production, relative to activin A.

Improved inhibin A production was accompanied by a substantial increase in the amount of $\alpha$-subunit precursor.

**Table 2.** Antibody Table

| Peptide/Protein Target | Antigen Sequence (if Known) | Name of Antibody | Manufacturer, Catalog Number, and/or Name of Individual Providing the Antibody | Species Raised (Monoclonal or Polyclonal) | Dilution Used |
|---|---|---|---|---|---|
| Inhibin $\beta$A-subunit | Binds residues 401-413 | E4 | Beckman Coulter/Oxford Brookes University (Oxford, UK) | Mouse, monoclonal | Specified in text |
| Inhibin $\alpha$-subunit | Binds residues 233-264 | R1 | Beckman Coulter/Oxford Brookes University (Oxford, UK) | Mouse, monoclonal | Specified in text |
| | | | Beckman Coulter/Oxford Brookes University (Oxford, UK) | | |

This 50-kDa species represents free α-subunit that has not dimerized with $\beta_A$-subunit and therefore has not been processed by proprotein convertases. Interestingly, the inhibin α-subunit is one of a small subset of TGF-β precursors that are cleaved at two distinct proprotein convertase motifs (33). The second cleavage site ($^{57}$RLPR$^{60}$) within the α-subunit precursor releases a 43-amino acid fragment that can limit inhibin activity (24). Recently we showed that processing at site$_2$ was absolutely required for the synthesis and secretion of inhibins A and B (24). Incorporating enhanced proprotein convertase cleavage sites at both site$_1$ and site$_2$ of the α-subunit led to a 9-fold increase in mature inhibin A production, ostensibly due to complete dimerization and processing of the α-subunit. Remarkably, enhanced inhibin production was accompanied by a 12.5-fold decrease in activin A levels. The production of inhibin B, relative to activin B, was similarly enhanced by the introduction of the supercleavage site in the α-subunit (data not shown). Thus, by incorporating improved cleavage sites within the α- and β-subunits, we have developed a regimen to produce high levels of bioactive inhibins.

Although our modifications had greatly improved the ratio of inhibin A to activin A produced by HEK293F cells, the remaining activin retained biological activity. Therefore, we incorporated a secondary mutation within the $\beta_A$-subunit (M418A). Met418 resides at the type I receptor (ALK4) interface of activin A, and we had previously shown that mutating this residue to alanine disrupted activin activity without affecting binding to ActRIIA/IIB (25). In the context of inhibin, the M418A $\beta_A$-subunit mutation did not affect expression of the SCUT variant but enhanced activity 8-fold. Because there was no change in inhibin-like activity after activin (M418A) removal, the increase in inhibitory activity of the inhibin preparation was primarily due to the inactivation of activin A. Thus, we can now produce inhibin A in the virtual absence of contaminating activin activity, which has long been the major obstacle to the use of inhibin as a therapeutic. Additionally, because the ALK4 binding site is conserved on the inhibin βB-subunit, this methodology will likely also aid the production of bioactive inhibin B.

The final modification incorporated into inhibin A was a HIS tag at the C terminus of the α-subunit prodomain. Mature inhibin A (M418A) was copurified using HIS affinity chromatography, indicating that it is secreted by HEK293F cells in a noncovalent complex with its prodomain (termed proinhibin A). This brings the number of TGF-β proteins shown to remain associated with their prodomains extracellularly to 13 (26–28, 33–35), suggesting this is the default manner in which these proteins are secreted from cells. For most family members, prodomains localize mature growth factors near target cells; however, the affinity of the interaction is not sufficient to suppress biological activity (26, 28). In contrast, the TGF-β isoforms, myostatin and growth differentiation factor-11, bind their prodomains with high affinity and are secreted from the cell in a latent form (33). In highly sensitive primary rat pituitary cells, proinhibin A had comparable activity to HPLC-purified mature inhibin A. However, in the less responsive LβT2 gonadotrope cell line, the presence of the prodomain increased inhibin activity greater than 20-fold. This correlated with an increased affinity of proinhibin A for betaglycan, suggesting that the prodomain facilitates inhibin binding to betaglycan. Mechanistically, we propose that the prodomain presents mature inhibin A to betaglycan (thereby increasing activity) but is then displaced, allowing the inhibin/betaglycan complex to bind and sequester activin type II receptors. The prodomain of cumulin (bone morphogenetic protein 15: growth differentiation factor-9 heterodimer) was recently shown to be indispensable for this growth factors positive effects on oocyte quality (34). Future studies will consider the effects of the prodomain on inhibin activity and half-life in vivo.

In conclusion, we have introduced a series of mutations into the α- and $\beta_A$-subunits that have increased mature inhibin A expression, dramatically decreased and inactivated contaminating activin A, and streamlined the purification process. It should now be possible to generate sufficient quantities of recombinant inhibin A to fully explore the considerable therapeutic potential of this molecule on bone and other tissues.

## Acknowledgments

We thank Justine Olcorn for the provision of the rat pituitaries for this study.

Address all correspondence and requests for reprints to: Kelly Walton, PhD, Hudson Institute of Medical Research, 27-31 Wright Street, Clayton, Victoria 3168, Australia. E-mail: kelly.walton@hudson.org.au.

This work was supported by Project Grant 1078879 from the National Health and Medical Research Council Australia. Hudson Institute of Medical Research is supported in part by the Victorian Government's Operational Infrastructure Support Program.

Disclosure Summary: The authors have nothing to disclose.

## References

1. **Woodruff TK, Besecke LM, Groome N, Draper LB, Schwartz NB, Weiss J.** Inhibin A and inhibin B are inversely correlated to follicle-

stimulating hormone, yet are discordant during the follicular phase of the rat estrous cycle, and inhibin A is expressed in a sexually dimorphic manner. *Endocrinology*. 1996;137:5463–5467.
2. **Robertson DM, Hale GE, Fraser IS, Hughes CL, Burger HG.** A proposed classification system for menstrual cycles in the menopause transition based on changes in serum hormone profiles. *Menopause*. 2008;15:1139–1144.
3. **Walton KL, Makanji Y, Wilce MC, Chan KL, Robertson DM, Harrison CA.** A common biosynthetic pathway governs the dimerization and secretion of inhibin and related transforming growth factor β (TGFβ) ligands. *J Biol Chem*. 2009;284:9311–9320.
4. **Wiater E, Vale W.** Inhibin is an antagonist of bone morphogenetic protein signaling. *J Biol Chem*. 2003;278:7934–7941.
5. **Massague J, Wotton D.** Transcriptional control by the TGF-β/Smad signaling system. *EMBO J*. 2000;19:1745–1754.
6. **Lewis KA, Gray PC, Blount AL, et al.** Betaglycan binds inhibin and can mediate functional antagonism of activin signalling. *Nature*. 2000;404:411–414.
7. **Wiater E, Lewis KA, Donaldson C, Vaughan J, Bilezikjian L, Vale W.** Endogenous betaglycan is essential for high-potency inhibin antagonism in gonadotropes. *Mol Endocrinol*. 2009;23:1033–1042.
8. **Perrien DS, Achenbach SJ, Bledsoe SE, et al.** Bone turnover across the menopause transition: correlations with inhibins and follicle-stimulating hormone. *J Clin Endocrinol Metab*. 2006;91:1848–1854.
9. **Perrien DS, Akel NS, Edwards PK, et al.** Inhibin A is an endocrine stimulator of bone mass and strength. *Endocrinology*. 2007;148:1654–1665.
10. **Perrien DS, Nicks KM, Liu L, et al.** Inhibin A enhances bone formation during distraction osteogenesis. *J Orthopaed Res*. 2012;30:288–295.
11. **Matzuk MM, Finegold MJ, Su JG, Hsueh AJ, Bradley A.** α-Inhibin is a tumour-suppressor gene with gonadal specificity in mice. *Nature*. 1992;360:313–319.
12. **Li Q, Kumar R, Underwood K, et al.** Prevention of cachexia-like syndrome development and reduction of tumor progression in inhibin-deficient mice following administration of a chimeric activin receptor type II-murine Fc protein. *Mol Hum Reprod*. 2007;13:675–683.
13. **Matzuk MM, Finegold MJ, Mather JP, Krummen L, Lu H, Bradley A.** Development of cancer cachexia-like syndrome and adrenal tumors in inhibin-deficient mice. *Proc Natl Acad Sci USA*. 1994;91:8817–8821.
14. **Harrison CA, Gray PC, Vale WW, Robertson DM.** Antagonists of activin signaling: mechanisms and potential biological applications. *Trends Endocrinol Metab*. 2005;16:73–78.
15. **Makanji Y, Temple-Smith PD, Walton KL, Harrison CA, Robertson DM.** Inhibin B is a more potent suppressor of rat follicle-stimulating hormone release than inhibin a in vitro and in vivo. *Endocrinology*. 2009;150:4784–4793.
16. **Duckert P, Brunak S, Blom N.** Prediction of proprotein convertase cleavage sites. *Protein Eng Des Sel*. 2004;17:107–112.
17. **Walton KL, Chan KL, Pruysers E, et al.** Use of detergent-based buffers allows detection of precursor inhibin forms in an immunoassay format. *Mol Cell Endocrinol*. 2013;381:106–114.
18. **Groome NP, Illingworth PJ, O'Brien M, et al.** Detection of dimeric inhibin throughout the human menstrual cycle by two-site enzyme immunoassay. *Clin Endocrinol (Oxf)*. 1994;40:717–723.
19. **Makanji Y, Harrison CA, Stanton PG, Krishna R, Robertson DM.** Inhibin A and B in vitro bioactivities are modified by their degree of glycosylation and their affinities to betaglycan. *Endocrinology*. 2007;148:2309–2316.
20. **Scott RS, Burger HG, Quigg H.** A simple and rapid in vitro bioassay for inhibin. *Endocrinology*. 1980;107:1536–1542.
21. **van Casteren JI, Schoonen WG, Kloosterboer HJ.** Development of time-resolved immunofluorometric assays for rat follicle-stimulating hormone and luteinizing hormone and application on sera of cycling rats. *Biol Reprod*. 2000;62:886–894.
22. **Wiater E, Harrison CA, Lewis KA, Gray PC, Vale WW.** Identification of distinct inhibin and transforming growth factor β-binding sites on betaglycan: functional separation of betaglycan co-receptor actions. *J Biol Chem*. 2006;281:17011–17022.
23. **Hertan R, Farnworth PG, Fitzsimmons KL, Robertson DM.** Identification of high affinity binding sites for inhibin on ovine pituitary cells in culture. *Endocrinology*. 1999;140:6–12.
24. **Walton KL, Kelly EK, Chan KL, Harrison CA, Robertson DM.** Inhibin biosynthesis and activity are limited by a prodomain-derived peptide. *Endocrinology*. 2015;156:3047–3057.
25. **Harrison CA, Gray PC, Fischer WH, Donaldson C, Choe S, Vale W.** An activin mutant with disrupted ALK4 binding blocks signaling via type II receptors. *J Biol Chem*. 2004;279:28036–28044.
26. **Harrison CA, Al-Musawi SL, Walton KL.** Prodomains regulate the synthesis, extracellular localisation and activity of TGF-β superfamily ligands. *Growth Factors*. 2011;29:174–186.
27. **Sengle G, Ono RN, Lyons KM, Bachinger HP, Sakai LY.** A new model for growth factor activation: type II receptors compete with the prodomain for BMP-7. *J Mol Biol*. 2008;381:1025–1039.
28. **Sengle G, Ono RN, Sasaki T, Sakai LY.** Prodomains of transforming growth factor β (TGFβ) superfamily members specify different functions: extracellular matrix interactions and growth factor bioavailability. *J Biol Chem*. 2011;286:5087–5099.
29. **Makanji Y, Walton KL, Wilce MC, Chan KL, Robertson DM, Harrison CA.** Suppression of inhibin A biological activity by alterations in the binding site for betaglycan. *J Biol Chem*. 2008;283:16743–16751.
30. **Constam DB.** Regulation of TGFβ and related signals by precursor processing. *Sem Cell Dev Biol*. 2014;32:85–97.
31. **Antenos M, Lei L, Xu M, Malipatil A, Kiesewetter S, Woodruff TK.** Role of PCSK5 expression in mouse ovarian follicle development: identification of the inhibin α- and β-subunits as candidate substrates. *PloS One*. 2011;6:e17348.
32. **Antenos M, Zhu J, Jetly NM, Woodruff TK.** An activin/furin regulatory loop modulates the processing and secretion of inhibin α- and βB-subunit dimers in pituitary gonadotrope cells. *J Biol Chem*. 2008;283:33059–33068.
33. **Shi M, Zhu J, Wang R, Chen X, Mi L, Walz T, Springer TA.** Latent TGF-β structure and activation. *Nature*. 2011;474:343–349.
34. **Mottershead DG, Sugimura S, Al-Musawi SL, et al.** Cumulin, an oocyte-secreted heterodimer of the transforming growth factor-β family, is a potent activator of granulosa cells and improves oocyte quality. *J Biol Chem*. 2015;290:24007–24020.
35. **Robertson IB, Horiguchi M, Zilberberg L, Dabovic B, Hadjiolova K, Rifkin DB.** Latent TGF-β-binding proteins. *Matrix Biol*. 2015;47:44–53.